Journal for ImmunoTherapy of Cancer

Preclinical and clinical evaluation of intratumoral injection of an IL-12 expressing SKV-012 oncolytic virus for advanced solid tumors

Zheng Jiang ,[1] Nian Yang,[2] Jing Jin,[1] Zongliang Zhang,[2] Huaqing Lu,[2] Long Xu,[2] Yongdong Chen,[2] Liyuan Jin,[3] Liangxue Zhou,[3,4,5] Hui Yang ,[6] Jun Liu,[6] Weiwei Zhang,[7] Aiping Tong ,[2,8,9] Xingchen Peng [1]

To cite: Jiang Z, Yang N, Jin J, *et al*. Preclinical and clinical evaluation of intratumoral injection of an IL-12 expressing SKV-012 oncolytic virus for advanced solid tumors. *Journal for ImmunoTherapy of Cancer* 2025;**13**:e011642. doi:10.1136/jitc-2025-011642

► Additional supplemental material is published online only. To view, please visit the journal online (https://doi.org/10.1136/jitc-2025-011642).

ZJ, NY and JJ contributed equally.

Accepted 19 May 2025

Check for updates

© Author(s) (or their employer(s)) 2025. Re-use permitted under CC BY-NC. No commercial re-use. See rights and permissions. Published by BMJ Group.

For numbered affiliations see end of article.

Correspondence to
Dr Xingchen Peng;
pxx2014@163.com

Dr Aiping Tong;
aipingtong@scu.edu.cn

ABSTRACT

Background SKV-012 is a novel engineered oncolytic virus (containing the viral neurovirulence ICP34.5 gene transcribed by the Survivin promoter with an upstream genetic component of interleukin-12 (IL-12) driven by the cytomegalovirus promoter) that preferentially replicates in tumors and helps stimulate antitumor immune responses.

Methods We evaluated SKV-012's safety and efficacy in preclinical models. In a phase I trial, patients with advanced solid tumors received intratumoral injections of escalating doses of SKV-012. Primary endpoints were safety and tolerability, while secondary endpoints were antitumor response and changes in the tumor microenvironment (TME), assessed by RECIST v1.1 criteria and multiplex immunohistochemistry and single-cell transcriptome analysis.

Results SKV-012-infected tumor cells secreted high levels of IL-12 and exhibited increased ICP34.5 expression. The combination of oncolytic herpesvirus and IL-12 was proven to reshape the TME by increasing the infiltration of immune cells, thereby significantly inducing immune cell-mediated cytolysis of tumor cells both in vitro and in animal models. Based on this, we then tested the safety, efficacy and immunogenicity of SKV-012 in patients with advanced solid cancers in a phase I clinical trial (NCT06080984). No dose-limiting toxicities were observed, and adverse events were mild. Three patients achieved partial responses; one had stable disease and two had progressive disease. SKV-012 altered the TME, increasing CD8+ T cells, conventional dendritic cells, and programmed death-ligand 1 expression.

Conclusions Intratumoral SKV-012 injections demonstrated a favorable safety profile and promising efficacy in animal models and patients with advanced cancers, thereby implicating its potential for clinical application in treatment-resistant advanced solid tumors.

WHAT IS ALREADY KNOWN ON THIS TOPIC

⇒ Oncolytic viruses (OV) are a promising cancer therapy that selectively replicate in and destroy tumor cells. OVs can be genetically engineered to express therapeutic genes, enhancing their antitumor effects and minimizing side effects.

WHAT THIS STUDY ADDS

⇒ Incorporating interleukin 12 (IL-12) expression into oncolytic herpes simplex virus can enhance its oncolytic potential, while Survivin can improve the safety and efficacy of OVs by controlling viral replication.

HOW THIS STUDY MIGHT AFFECT RESEARCH, PRACTICE OR POLICY

⇒ This study implicates that the genetically modified OV with IL-12 expression is effective in various types of solid cancer treatment and carries great potential for clinical transformation.

INTRODUCTION

Oncolytic viruses (OVs) epitomize an emerging category of cancer therapeutics, employing either unaltered or genetically engineered viral agents, thereby offering the benefits of selective replication in tumor cells, delivery of multiple eukaryotic transgene payloads, induction of immunogenic cell death and promotion of antitumor immunity, and a tolerable safety profile that largely does not overlap with that of other cancer therapeutics. The genesis of this approach traces back over a century, when it was initially observed that patients with cancer exhibited regression of malignancies following viral infections.[1] Mechanistically, specific viral strains have been harnessed for their proclivity to selectively replicate within tumor cells while sparing their normal counterparts, thereby executing tumor cell lysis through viral replication.[2] Several viruses, including herpes simplex virus (HSV), vaccinia virus, adenovirus, and reovirus, have demonstrated notable oncolytic potential in both preclinical experiments and clinical trials.[3] As technological prowess advances, the advent of recombinant DNA technology has furnished vital instruments for the exploration of

viral biology, thereby propelling the domain of biological cancer therapy into a new era of therapeutic innovation. Contemporary iterations of OVs are frequently engineered to express immunostimulatory proteins, concomitantly serving as viral vectors. These tailored viral constructs exhibit enhanced selectivity for tumor cells and diminished systemic toxicity, thus underscoring their substantial promise in cancer treatment.

HSV represents a highly lytic viral species, where the elimination of the extensively investigated infected cell protein 34.5 (ICP34.5)-encoding gene imparts tumor selectivity. The ICP34.5-deleted HSV exhibits a propensity to infect and replicate within a broad spectrum of human tumor cells, seemingly irrespective of the genetic anomalies underpinning their oncogenic transformation.[2] Consequently, HSV holds the potential to serve as a valuable OV applicable to the treatment of a diverse array of solid tumor types. A pre-eminent exemplar of the most widely employed HSV-based OV is talimogene laherparepvec (T-VEC). T-VEC is an engineered HSV-1 variant featuring the incorporation of the granulocyte monocyte colony-stimulating factor gene, coupled with the deletion of the ICP34.5 and ICP47 genes. This strategic genetic modification ensures an abortive infection within normal cells, thereby conferring cancer cell-specific replication potential. Additionally, it facilitates immune-mediated viral clearance in normal cells, while concurrently augmenting the cell surface expression of MHC-I molecules in cancer cells.[4 5] Remarkably, T-VEC stands as the pioneering OV to have received Food and Drug Administration (FDA) approval for melanoma therapy.[6 7] However, in those more recent phase III clinical trials, T-VEC single drug was only able to achieve a durable response rate of 19.3%; an objective response rate of 31.5%; and a disease control rate of 76.3%, with median overall survival of 23.3 months in the treatment of advanced melanoma.[8] However, besides advanced melanoma, T-VEC is somehow not as effective in head and neck squamous cell carcinoma (HNSCC) as indicated by the MASTERKEY-232 trial, where the efficacy with the combination was similar to that with pembrolizumab monotherapy.[9] Also, in another phase I clinical trial involving various types of solid tumors, the T-VEC failed to elicit any partial responses (PR) or complete responses (CR) in participants.[2]

To achieve better therapeutic outcomes, researchers started to further modify the OVs to express therapeutic genes for multiple mechanisms of action.[10] Various types of transgenes can be inserted into OVs, encompassing the TRAIL gene, which mediates tumor cell apoptosis or necrosis,[11] or genes coding various cytokines like interleukin 2 (IL-2), IL-12 and IL-15, which are closely associated with immune response.[12–14]

While proinflammatory cytokines can stimulate potent antitumor immunity and transform a cold tumor microenvironment (TME) into a hot one, their clinical use is often limited by significant side effects and unfavorable pharmacokinetics.[15] IL-12, as a cytokine with stimulatory effects on helper T lymphocytes, cytotoxic T lymphocytes (CTLs), and natural killer (NK) cells,[16] is able to elicit significant antitumor effects when delivered to the TME.[17] It can also inhibit angiogenesis in tumor tissue.[18] Multiple preclinical studies have demonstrated that IL-12 therapy can generate systemic, adaptive immunological memory capable of controlling local tumor lesions and inhibiting metastases[19 20]; however effective, the adverse effects triggered by IL-12, like gastrointestinal dysregulation, liver toxicity, hematological toxicity and even mental conditions, should not be ignored and should be tried to be avoided.[21]

Survivin, encoded by the BIRC5 gene, is a member of the inhibitor of apoptosis protein family and plays a crucial role in regulating cell division and inhibiting apoptosis, while the overexpression of Survivin is associated with tumor progression.[22] The Survivin can be used as a tumor-specific promoter to control the expression of virulence gene ICP34.5, thus enabling the specific viral replication and virulence inside the tumor while sparing the normal tissue.[23] OV with similar design using nestin as the tumor-specific promoter has demonstrated a preferred safety and efficacy profile in a phase I clinical trial on glioblastoma.[24]

Here, we report SKV-012, a novel engineered multifunctional oncolytic HSV-1. Tumor-specific promoter-mediated attenuation strategy that allows for selective oncolysis of tumor cells, while sparing healthy tissue, was coupled with the expression of IL-12 transgene (figure 1). IL-12 drives Th1 transformation of the TME, leading to interferon gamma (IFN-γ) and cytotoxic T-cell-dependent antitumor immunity.[25] The selective enhancement of viral replication within tumors amplifies oncolysis and significantly boosts IL-12 expression, further augmenting the therapeutic efficacy. The preclinical experiments have demonstrated favorable safety and efficacy profiles. Thereafter, we designed and conducted a phase I (NCT06080984), open-label, dose-escalation study of intralesional SKV-012 to determine the safety and efficacy of the therapy and define a recommended phase II dose.

MATERIALS AND METHODS

Construction of OV SKV-012

The generation of the attenuated oncolytic herpesvirus (oHSV) (an OV derived from HSV type 1 (CCTCC No: V202271) with deletions in both the endogenous ICP34.5 gene and the ICP47 gene) has been previously described.[26] Briefly, a transcriptional cassette consisting of a murine or human IL-12 (hIL-12) transcriptional unit driven by the cytomegalovirus (CMV) promoter, along with optimized sequences of key virulence factor ICP34.5 under the transcriptional control of the Survivin core promoter (online supplemental table S1), was inserted into the deleted ICP34.5 locus. IL-12 transcriptional units were combined in one sequence with G_4S linkers between the IL-12B and IL-12A subunits. The IL-12B (UniProt mouse P43432 and

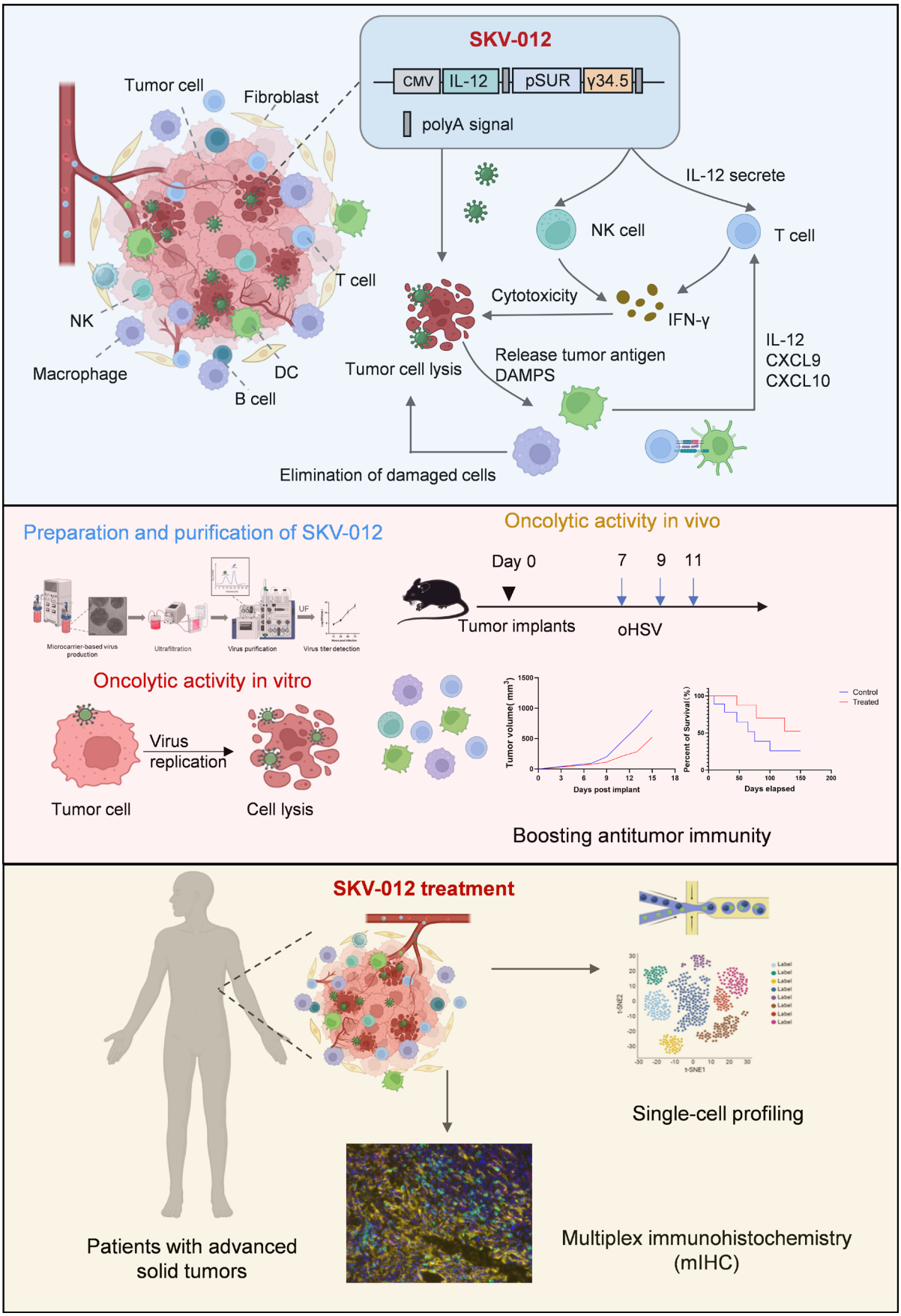


Figure 1 Schematic illustration of the design and mechanism of SKV-012 in advanced solid tumor treatment (created with BioRender.com). CMV, cytomegalovirus; DC, dendritic cell; IFN-γ, interferon gamma; IL, interleukin; NK, natural killer; oHSV, oncolytic herpesvirus, CXCL, C-X-C motif chemokine ligand, DAMPS, damage-associated molecular patterns.

human P29460) signal peptide was retained for secretion, and the IL-12A signal peptide was removed (first 22 amino acids for mouse and human, UniProt mouse P43431 and human P29459). This cassette was then constructed into oHSV by using the CRISPR/Cas9 system as previously described.[26] All modifications were confirmed by Sanger sequencing.

SKV-012 manufacture

The SKV-012 was manufactured from oHSV-infected Vero cells. Vero cells were grown on 3D TableTrix (CytoNiche) microcarriers for 48 hours in a 3D FloTrix miniSPIN FLEX 4 (CytoNiche). The final cell density was approximately 2 500 000 cells/mL at which point cells were infected with SKV-012 and harvested at 72 hours after infection. Clarification of harvested cells was achieved by microfiltration (MF). Benzonase was applied after MF and before column purification. The SKV-012 was purified using Capto Core 700 (Cytiva) and then concentrated to a high viral titer. The purified oHSV is then titrated on Vero cells, and virus titers are calculated by TCID50 assays. The processing and storage of SKV-012 are presented in appendix C of the prior publication for preparation guidelines.[27]

Cells

Two human melanoma A375 and UACC62, human osteosarcoma 143B, human glioblastoma U-87MG, human umbilical vein endothelial cell (HUVEC), mouse colon carcinoma CT26, mouse melanoma B16-F10, and monkey kidney epithelium Vero cell lines were used in cell experiments or animal models in the preclinical study. A375, 143B, U-87MG, B16-F10, HUVEC, CT26, and Vero cell lines were purchased from American Type Culture Collection (ATCC). UACC62 cell lines were validated for expression of melanocytic/pigmentation differentiation markers.[28] The cell lines were cultured in complete cell medium with 10% fetal bovine serum (FBS) and 100 U/mL penicillin-streptomycin. B16H (B16-F10-HVEM) cells were generated by lentiviral vector transduction of herpesvirus entry receptor HVEM transcript (UniProtKB Accession No Q92956). Subsequently, A375, UACC62, and 143B cell lines were lentivirally transduced to express firefly Photinus pyralis luciferase reporter proteins to measure cytotoxicity.

Peripheral blood mononuclear cells (PBMC) were derived from anonymous blood donors and subjected to density gradient centrifugation using Ficoll (GE Healthcare). All procedures were approved by the clinical research ethics committee of Sichuan University (Chengdu, China). PBMCs were cultured in complete T cell medium (X-vivo medium, Lonza) supplemented with Glutamax+10% of heat-inactivated FBS+100 U/mL penicillin-streptomycin.

Animals and mouse cytokine assay

All animal experiments were approved by and performed under the guidance of the Institutional Animal Care and Use Committee of Sichuan University (Chengdu, China). Mice were purchased from GemPharmatech (Nanjing, China) and maintained at specific pathogen-free conditions. Female mice at 6–8 weeks of age were used for all experiments. The experimental details are described in the corresponding figure legends and the online supplemental information.

The cytokine assay was conducted using mouse IL-7 (217-17-10UG, Gibco), IL-12 (210-12-10UG, Gibco), and IL-15 (210-15-10UG, Gibco). The concentrations of mouse IL-12 in tumor tissue were quantified by ELISA kit (ELK Biotechnology, ELK9395) according to the manufacturer's protocol and analyzed on a SpectraMax iD5 reader.

Flow cytometry analysis

Antibodies used for flow cytometry (FCM) are cataloged in online supplemental table S2. Survivin antibody (Proteintech) was used to detect the expression of Survivin on A375, UACC62, and 143B cells. Single-cell suspensions from tumors were blocked with human TruStain FcX (BioLegend) and intracellularly stained using BD Pharmingen Transcription Factor Buffer Set (BD Biosciences Pharmingen) according to the manufacturer's protocol.

For TME analysis, B16-HVEM syngeneic tumors were digested into single-cell suspensions by Collagenase type IV (Sigma-Aldrich) and DNase-I (Roche), and a 70 µm cell strainer (BD Falcon) was used to filter the tumor digests, and then blocked by CD16/CD32 antibody (BioLegend), and dead cells were excluded by a Zombie NIR Fixable Viability Kit (BioLegend). The following antibodies used in FCM were purchased from BioLegend and BD: anti-mouse CD45-PerCP (BioLegend), anti-mouse CD3-BV605 (BioLegend), anti-mouse CD8a-BV510 (BioLegend), anti-mouse CD4-FITC (BD), anti-mouse FOXP3-PE (BioLegend), anti-mouse NK1.1-APC (BioLegend), anti-mouse/human CD11b-FITC (BioLegend), anti-mouse I-A/I-E-BV421 (BioLegend), anti-mouse Gr-1-BV510 (BioLegend), and anti-mouse F4/80-PE (BioLegend). Anti-mouse CD206-APC was purchased from BD. FCM experiments were performed using a Beckman Coulter Cytoflex flow cytometer or LSR Fortessa cytometer (BD). FlowJo and CytExpert software were used for cytometry data analyses.

Luciferase assay

Construction of pGL3-Survivin

Survivin core promoter (−255 to 0) was cloned into the multiple cloning sites of pGL3-Basic (Addgene, Plasmid No 212936) upstream of the firefly luciferase gene with primers flanked with MluI or XhoI sites to create pGL3-Survivin.

Reporter assays

U87, A375, UACC-62, 143B, and HUVEC cells were seeded at a density of 10^5 cells in a 12-well format. Cells were transfected the following day using Polyethylenimine (MedChemExpress) with 1.35 µg of the pGL3-Survivin

and 0.15 µg of pRL-TK (Promega), a control Renilla luciferase vector. 48 hours later, cells were lysed and luciferase activity was assayed with the Dual Luciferase Reporter (Promega) assay in a 96-well format according to manufacturer instructions. Experiments were performed in triplicate wells. Relative luciferase activity was calculated as the ratio of firefly to Renilla luciferase activity, to control transfection efficiency.[25] Control is the relative luciferase activity of cells transfected with promoterless reporters alone (pGL3-Basic).

Luciferase-based cytotoxicity assay

A total of 10^4 target tumor cells were cocultured with SKV-012 [MOI (Multiplicity of infection)=0.1] and PBMC or conditioned medium at the different effector-to-target ratios for 72 hours based on the experimental setting, and the target/effector cocultures were subjected to luciferase activity measurement to determine the residual target tumor cells at the endpoint according to the Luciferase Assay System (Promega) protocol. The luciferase signal generated by the remaining tumor cells was acquired by SpectraMax iD5. The percentage of target lysis was determined using the formula: [(luminescence tumor only)−(luminescence tumor infected by SKV-012+PBMC)]/(luminescence tumor only)×100%.[29]

Clinical trial design

This study primarily included patients with histologically or cytologically confirmed advanced solid malignant tumors including HNSCC, melanoma and soft tissue sarcomas. For patients with confirmed advanced HNSCC, they should have met the following criteria: had failed standard second-line treatment and tumor cannot be cured through local treatment (surgery or definitive radiation therapy). For patients with stage III and IV malignant melanoma, they should have failed at least two lines of standard treatment (including chemotherapy, immunotherapy or targeted therapy). In addition, for patients with stage III malignant melanoma, they should also not be eligible for surgical resection. For patients with advanced soft tissue sarcomas, the tumor should be either locally unresectable or metastatic, and the patient should have failed prior systemic treatments.

Patients should be older than 18 years; had expected survival ≥3 months; had an Eastern Cooperative Oncology Group (ECOG) performance status of 0–1; had the last chemotherapy/radiotherapy/surgery more than 28 days; acute toxic effects of prior chemotherapy, radiotherapy, or surgical procedures had to have resolved to Common Terminology Criteria for Adverse Events (CTCAE, version 5.0) grade ≤1; had adequate hepatic, renal, cardiac and bone marrow function (hemoglobin ≥90 g/L (without blood transfusion in the last 14 days); neutrophil count >1.5×10^9/L; platelet count ≥80×10^9/L; total bilirubin ≤1.5×ULN (upper limit of normal); alanine aminotransferase (ALT) or aspartate aminotransferase (AST) ≤2.5×ULN); if there was liver metastasis, ALT or AST≤5×ULN; estimated glomerular filtration rate ≥60 mL/min (Cockcroft-Gault formula); had at least one injectable lesion (those suitable for direct injection or injection with the assistance of medical imaging) defined as follows: at least one injectable lesion in the skin, mucous membrane, subcutaneous tissue, or lymph node with a longest diameter ≥10 mm, or multiple injectable lesions with a total longest diameter ≥10 mm.

The main exclusion criteria were prior participation in another drug clinical trial within the past 4 weeks; tumor located near major blood vessels; had poorly controlled heart disease (New York Heart Association class III or IV); patients were currently pregnant or breastfeeding; with known HIV, hepatitis B, or hepatitis C infections; had active immunosuppressive therapy; had history of substance abuse; had diseases requiring the use of drugs against HSV, like acyclovir; and unable to give informed consent.

Dose-escalation design followed the traditional '3+3' design (online supplemental figure S6). Cohorts of three patients received virus injection into the target lesion using a dose-escalation schedule: 10^6 pfu/mL (cohort 1); 10^8 pfu/mL (cohort 2). The intratumoral injection was performed directly for cutaneous or subcutaneous lesions, or with ultrasound/CT guidance for deep-situated lesions. The volume of the agent was determined according to the tumor volume (diameter ≤1.5 cm, maximum of 1 mL; diameter 1.5–2.5 cm, maximum of 2 mL; diameter greater than 2.5 cm, maximum of 4 mL). Each injection was spread out into multiple locations within the tumor. The viral agent was given at 2-week intervals.

Observational endpoints

The maximum tolerated dose was identified as the dose level before the occurrence of dose-limiting toxicities (DLTs) in two or more patients. The severity of any adverse events (AEs) was graded in accordance with the National Cancer Institute CTCAE version 5.0. DLT was defined as any of the following events within the first 4 weeks after the initial dose that was deemed treatment related by the investigators: hematological toxicities including grade 4 neutropenia, grade 3 or higher febrile neutropenia (defined as a neutrophil count below 1.0×10^9/L with a single temperature above 38.3°C, or a temperature of 38.0°C or higher sustained for more than 1 hour), grade 4 thrombocytopenia, grade 3 thrombocytopenia with bleeding, and grade 4 anemia. Non-hematological toxicities of grade 3 or higher were also considered, with certain exceptions. These exceptions were: nausea, vomiting, diarrhea, fatigue, edema, and hyperglycemia that improved to grade 2 or lower within 3 days with supportive treatment; grade 3 infusion reactions or fever lasting no more than 6 hours, treatable with physical cooling or supportive measures; and grade 3 skin toxicity that improved to grade 2 or lower within 7 days with supportive treatment.

Target and non-target lesion assessments were conducted at screening, 28 days after the initial dose, and then every 6–8 weeks until disease progression or death.

Radiographic assessments were performed using contrast CT or MRI. The response is evaluated using RECIST v1.1.

Laboratory tests

Viral shedding

Quantitative PCR (qPCR) tests were conducted on patients' blood, urine, injection site dressings, saliva, and stool to monitor viral shedding and were collected 4 hours, 2 days, and 7 days after the injection, and then before every subsequent injection until the first radiological evaluation. qPCR was performed according to previously described methods for HSV shedding detection[30]; detailed procedures were included in the online supplemental file along with online supplemental table S1.

Anti-HSV antibody assay

Within 14 days before the first injection, baseline anti-HSV antibody levels against the OV were measured. During the first dose, blood samples were collected 4 hours, 2 days, and 7 days after the injection, and then before every subsequent injection to monitor anti-HSV antibody levels until the first radiological evaluation. Anti-human HSV-I immunoglobulin G titers were determined by ELISA from patient serum samples according to manufacturer's instructions (CSB-E08997h; CUSABIO). Results were the optical density values at 450 nm.

Cytokines

IFN-γ and IL-12p70 were measured within 14 days before the first injection. During the first dose injection, blood samples were collected 4 hours, 2 days, and 7 days after the injection, and then before every subsequent injection until the first radiological evaluation. The concentrations of cytokines in serum were sent to the laboratory of West China Hospital for quantification.

T, B, and Natural Killer cell

T, B, and Natural Killer (TBNK) cell proportion was evaluated along with the radiographic evaluation at screening and 28 days after the initial dose.

Single-cell RNA sequencing

Biopsy samples were collected from all patients before treatment initiation and again at the 6-week mark. During the quality filtering step, genes that were not expressed in at least 40 cells were labeled as low quality and excluded from downstream analysis. Additionally, raw count matrices were filtered by removing cell barcodes with fewer than 200 expressed genes. As a result, a total of 66 355 high-quality cells were obtained. Only samples meeting the criteria for adequate cell count and viability were included in the final analysis. The gathering and analysis of the data were done with the researcher blinded to the patients' information. The usual manufacturer's protocol (CG000206 RevD) was followed for all subsequent steps, including the building of the library. The libraries were sequenced using 2×150 chemistry on an Illumina NovaSeq6000. For RNA-seq data processing on a single cell with default and suggested parameters, reads were processed using the Cell Ranger 7.0.1 pipeline. Next, R (V.4.3.0) was used to import the clustered data and conduct additional analysis. The filtered raw count matrix was further analyzed using the Seurat (version 4.0) R package for integration of single-cell RNA-seq data for quality control and downstream analysis. Cells with fewer than 200 or more than 6000 identified genes were disregarded. Cells expressing more than 10% of the mitochondrial genes were eliminated in order to exclude low-viability cells. Next, using t-distribution stochastic neighborhood embedding (t-SNE), we created a 2D map to depict the clustering after performing principal component analysis. We used identical scaling, dimensionality reduction, and clustering processes for subclustering on that particular batch of data. We found significantly differentially expressed genes for each cluster by comparing it to the other clusters using the Wilcoxon rank-sum test. Cell type was determined using SingleR and recognized marker genes. Potential intercellular communication was calculated and plotted using CellChat version 1.1.3. Developmental pseudo-time and cell trajectory analysis was performed by the Monocle 2 package (version 2.28.0) 60 to infer the development of the indicated cells.

Multiplex immunohistochemistry

Formalin-fixed paraffin-embedded 5 µm tissue sections from the experimental mice—including pretreatment biopsy, week 6 biopsy and resected tumor samples—were stained using the IRISKit HyperView multiplex immunostaining kit (Catalog No MH900205, MH900206) according to manufacturer's instructions. The slides were imaged using an Olympus VS200 slide scanner and further analyzed using QuPath software V.0.4.4. Enumeration of positive cells per square millimeter of tissue was calculated to provide a density of positive cells across the entire tissue section. The antibodies used included rabbit monoclonal CD3 (Catalog No 78588, Cell Signaling Technology), F4/80 (Catalog No 70076, Cell Signaling Technology), Arginase-1 (Catalog No 93668, Cell Signaling Technology), αSMA (Catalog No ET1607-53, HUABIO), CD68 (Catalog No 76437, Cell Signaling Technology), CD163 (Catalog No 93498, Cell Signaling Technology), CD11c (Catalog No 45581, Cell Signaling Technology), CD8 (Catalog No 85336, Cell Signaling Technology), CD4 (Catalog No 48274, Cell Signaling Technology), Foxp3 (Catalog No 98377, Cell Signaling Technology), recombinant PD-L1 (Catalog No ab228462, Abcam), recombinant Ki67 (Catalog No ab16667, Abcam), and recombinant mouse monoclonal pan Cytokeratin (Catalog No HA601138, HUABIO).

Statistical analysis

Patient characteristics, clinical outcomes, and safety were presented using descriptive statistics. The safety profile was assessed as the primary outcome. Standard RECIST v1.1 guidelines were applied for the analysis of all clinical responses. Treatment responses, as secondary

outcomes, including CR, PR, stable disease (SD), progressive disease (PD), and the duration of responses, were analyzed descriptively. Wilcoxon rank-sum test was used for between-cluster comparison in gene expression.

RESULTS

Therapeutic potential of oHSV with cytokines in immunocompetent mouse models

To improve oHSV antitumor effectiveness and ultimately better clinical outcomes in patients, we established two syngeneic mouse models by subcutaneously injecting 5×10^6 murine tumor cells: B16H (with herpesvirus entry receptor HVEM overexpression) and CT26 to systematically assess the combination strategies of oHSV (an OV derived from HSV type 1 (CCTCC No: V202271) with deletions in both the endogenous ICP34.5 gene and the ICP47 gene) with cytokines, including IL-7, IL-12, and IL-15 (figure 2A). After tumor volume reached about 100 mm3, animals received three intratumoral injections of oHSV, oHSV+IL-7, oHSV+IL-12, oHSV+IL-15, or phosphate buffered saline (PBS) as a placebo control (each injection carried 50 ng of cytokine). oHSV combined with IL-12 significantly inhibited tumor growth when compared with groups after three injections into tumors (figure 2B). Moreover, oHSV+IL-12 and oHSV+IL-15-treated tumors were regressed within 10–14 days after the last virus injection. To confirm our findings, we repeated the above experiment with some modifications: performing two administrations of all groups and sacrificing the mice on day 12 to determine the intratumoral infiltration of T cells, NK cells, macrophages, CD8+ T cells, and Tregs by FCM (online supplemental figure S1). Combination of oHSV and IL-12 reshaped the immune microenvironment and increased immune cell infiltration, especially T cells and NK cells in B16H and T cells in CT26 tumor models (figure 2C and online supplemental figure S2). Although the combinations of IL-7, IL-15, and oHSV also increased immune cell infiltration, oHSV+IL-12 showed therapeutic outcomes superior to other combinations. Thus, we opted for oHSV+IL-12 as a promising combination strategy for developing a novel OV for improving clinical outcomes in patients in our study.

Mice treated with oHSV+cytokine dual therapy exhibited varying responses in B16H tumors. The cure rates for the 'PBS', 'oHSV', 'oHSV+IL-7', 'oHSV+IL-12', and 'oHSV+IL15' groups were 0%, 0%, 0%, 100%, and 60%, respectively, 60 days after tumor inoculation. However, in the CT26 tumor-bearing mouse model, only the oHSV+IL-12 treatment group achieved a 40% cure rate, while all other groups showed a 0% cure rate. As a result, the CT26 model was excluded from the rechallenge (data not shown).

Then, we conducted a tumor rechallenge experiment on the complete responders from the oHSV+IL-12-treated B16H tumor-bearing mice, as shown in figure 2. 80% of the surviving animals in this treatment group were protected against the subsequent rechallenge on day 60, indicating long-term immunity against tumor. These data have been incorporated into online supplemental figure S2B.

SKV-012 enhances antitumor immunity in vitro

To improve oHSV cytotoxic and immunomodulatory features, we recovered the key virulence factors by using a new truncated 225 bp Survivin promoter. Survivin expression profiles across tumor samples and paired normal tissues were generated by the GEPIA database (figure 3A and online supplemental figure S3). Survivin was strongly expressed in many different tumor tissues but has limited expression at low levels in normal tissues. Furthermore, we also validated the expression of Survivin in tumors, including melanoma and osteosarcoma, by using FCM and immunohistochemistry (figure 3B,C). Although deletion of the neurovirulence factor ICP34.5 has improved the virus vector safety, especially for the treatment of patients with glioma, its inactivation has been shown to cause insufficient cell lysis in TME. We hypothesized that Survivin promoter remodeling to express ICP34.5 might augment virus replication. To test this hypothesis, we first used a reporter assay system in which the relevant portion of the Survivin core promoter (−225 to 0) was cloned upstream of the firefly luciferase gene. Compared with PGL3-Basic, the Survivin truncated promoter conferred increased transcriptional activity in four distinct tumor cell lines and limited transcriptional activity in one normal cell line (figure 3D). Thus, we designed an innovative OV expressing an IL-12 driven by the CMV promoter, and codon optimization of ICP34.5 driven by the Survivin truncated promoter, and characterization of SKV-012 (figure 3E,F). The concentrations of hIL-12 secreted from SKV-012-infected tumor cell supernatants were quantified by ELISA (figure 3G). We next determined the virus replication by virus yield assay (number of progeny virions generated from cell infection) (figure 3H).[24] To investigate the antitumor activity of SKV-012-mediated cell lysis and cytotoxicity in vitro, we conducted a luciferase-based killing assay by coculturing human PBMCs with A375, UACC62, and 143B tumor cells (which were previously transduced with luciferase) at the concentration ratio of 4:1, 2:1 and 1:1, respectively. Tumor cells were precultured for 12 hours in the presence or absence of OV, then added PBMC to the wells. After 72 hours of coculture, estimation of cell lysis and cytotoxicity were assessed by measuring luminescence. Noticeably, SKV-012 significantly induced immune cell-mediated cytolysis when compared with an uninfected control (figure 3I).

SKV-012 is safe and elicits durable and protective antitumor responses

Consistent with the T-VEC and G47Δ prescribing regimen,[31 32] we conducted safety assessments in 3-week-old Bagg Albino/c (BALB/c) mice. Mice were inoculated subcutaneously in the flank with either a

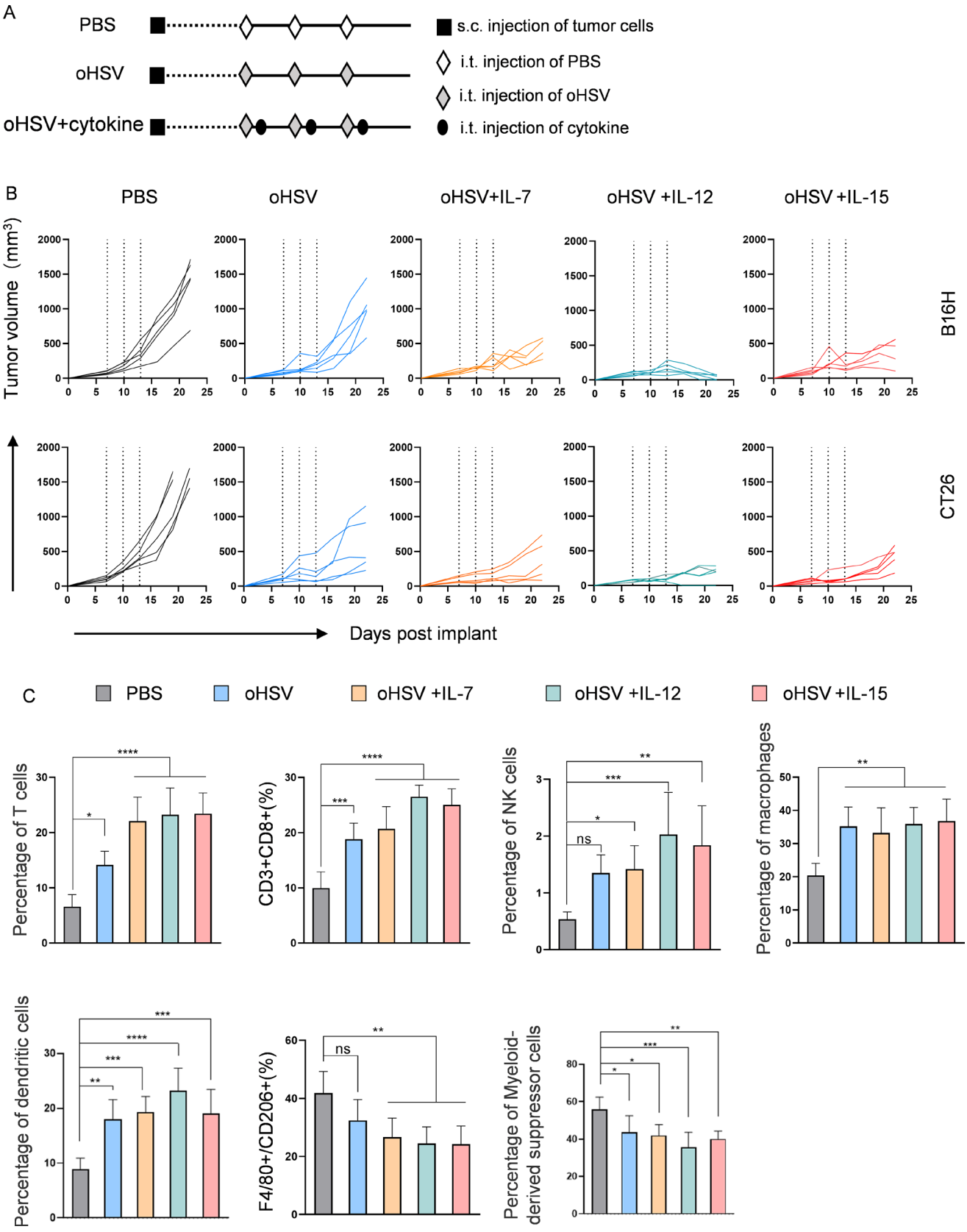


Figure 2 In vitro antitumor efficacy evaluation. (A) Schematic representation of the oncolytic virus-cytokine combination. (B) Tumor growth curves of animals after treatment with oHSV, oHSV plus cytokine, or control. Animals received intratumoral injections of 10^6 pfu oHSV and 50 ng cytokine two times per week. Dashed vertical lines represent dosing days. (C) Immunological infiltration features in B16H tumors (n=5). One-way analysis of variance (ANOVA) was used for statistical analysis, and Dunnett's method was used for multiple comparison correction of p values (n=5). ****P<0.0001, ***p<0.001, **p<0.01, *p<0.05; ns, p>0.05. IL, interleukin; NK, natural killer; oHSV, oncolytic herpesvirus.

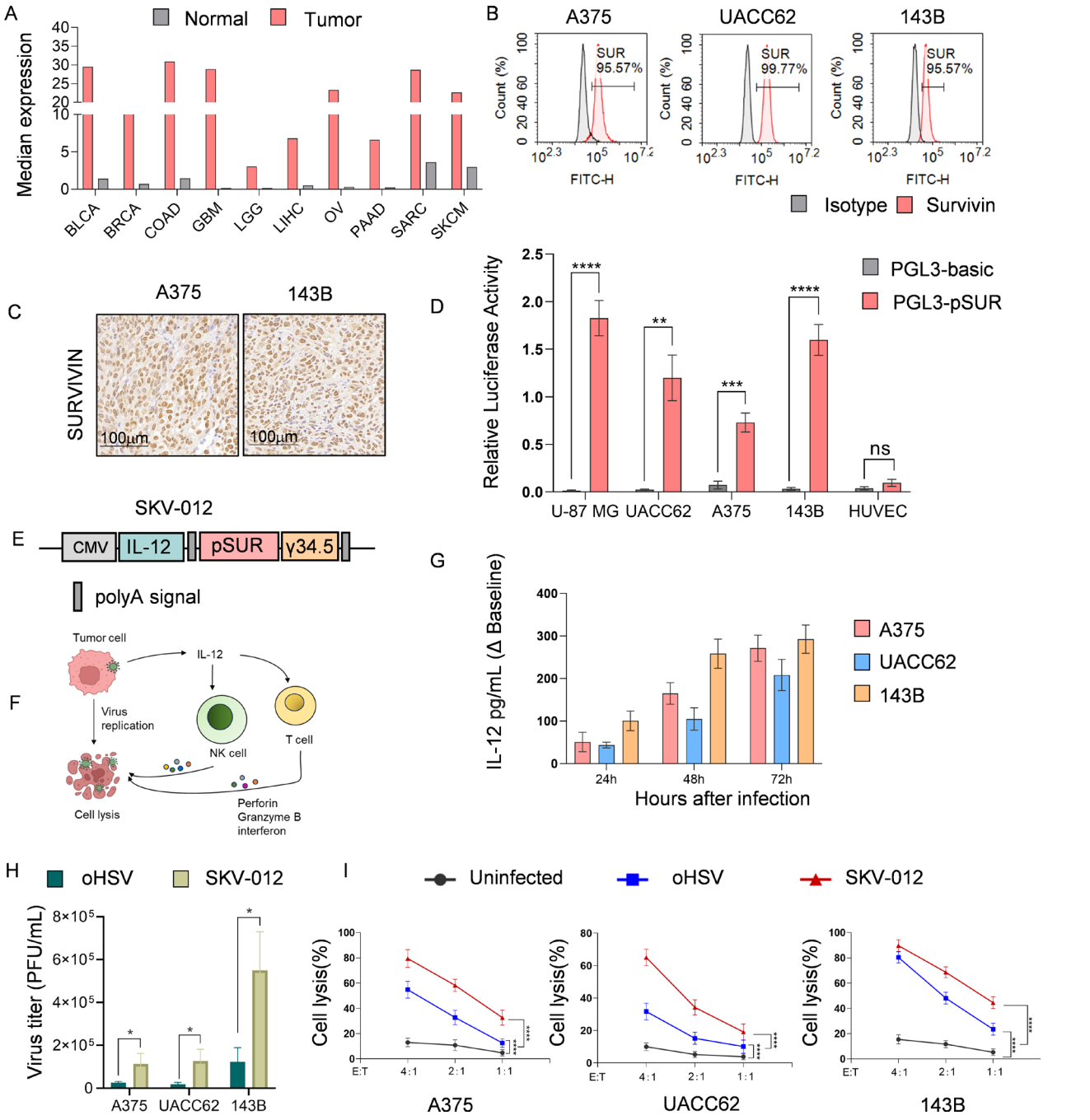


Figure 3 Design and testing of the SKV-012 oncolytic virus. (A) Gene expression profiles of tumor and paired normal tissues (generated by GEPIA database). (B) Representative histograms of flow cytometric analysis of Survivin expression on human tumor cells measured. (C) Immunohistochemistry (IHC) analysis of Survivin expression. Tissue slides were from tumor tissues isolated from experimental mice. (D) Transcriptional activity of the Survivin core promoter (−255 to 0) was detected by luciferase reporter assay compared with the vector PGL3-Basic in U87, A375, UACC62, 143B, or HUVEC cell lines. Values represent mean±SEM, representative of n=3 independent experiments. (E) Gene map of oncolytic viruses (OVs) used in this study. SKV-012 deleted two copies of γ34.5 and inserted the IL-12 gene driven by the CMV promoter and γ34.5 driven by the Survivin core promoter. (F) Schematic diagram of the antitumor effect of SKV-012. (G) Expression of IL-12 in culture supernatants after infected with 10^3 pfu of SKV-012. The supernatant culture medium of the uninfected tumor cells as a baseline. Values represent mean±SEM, representative of n=3 independent experiments. (H) A375, UACC62, and 143B cells were infected with 10^3 pfu of either oHSV or SKV-012. Titers of each sample were determined 3 days after infection. Values represent mean±SEM, representative of n=3 independent experiments. (I) Cytotoxicity and cell lysis mediated by SKV-012 were assessed by luciferase-based specific lysis assay. Tumor cells were treated with oHSV, SKV-012, or uninfected conditioned medium at varying effector to target (E:T) ratios. Values represent mean±SEM, representative of n=3 independent experiments. (D, H) Multiple unpaired t-test. (I) Two-way analysis of variance (ANOVA) with Tukey's multiple comparison tests. ****P<0.0001, ***p<0.001, **p<0.01, *p<0.05; ns, p>0.05. CMV, cytomegalovirus; HUVEC, human umbilical vein endothelial cell; IL, interleukin; NK, natural killer; oHSV, oncolytic herpesvirus.

single high dose (1×10^9 pfu of SKV-012) or multiple high doses (1×10^9 pfu administered every other day for a total of three doses). No adverse effects were observed, thereby supporting the safety profile of SKV-012.

To comprehensively evaluate the antitumor efficacy of SKV-012 in vivo, we used a previously described two syngeneic mouse models created by subcutaneous injection of 5×10^6 CT26 and B16H tumor cells into BALB/c and C57BL6 mice, respectively (figure 4A). The two mouse models received three injections of SKV-012 (murine IL-12) at a dose of 10^6 pfu. SKV-012 significantly slowed tumor progression compared with oHSV group without significant weight loss (figure 4B, online supplemental figure S4A). SKV-012 significantly prolonged median survival compared with both PBS control and oHSV treatment (figure 4C,D). Additionally, in the evaluation of the SKV-012 animal efficacy model, rechallenge experiments were performed on cured mice, as shown in figure 4D and online supplemental figure S4C. SKV-012 can induce long-term tumor-specific immunological memory and has the most profound effect on preventing tumor regrowth (online supplemental figure S4D).

Additionally, IL-12 levels in peripheral blood were assessed by ELISA in the tumor-bearing mouse model used in online supplemental figure S4B. However, IL-12 levels were below the detection limit in the tested samples. In the CT26 and B16H models, intratumoral administration of SKV-012 led to secretion of murine IL-12 (we also determined the murine IL-12 expression in vitro, data not shown) in the injected tumors (online supplemental figure S4B). The multiplex immunohistochemistry (mIHC) analysis 48 hours after completing two injections demonstrated increases in the density of CD3+ T cells and F4/80+ macrophages (figure 4E). We repeated the experiments with the xenotransplantation mouse models by using nude mice subcutaneous injection of human tumor cell A375 or 143B, but without infusing PBMCs and activated T cells. We observed that in nude mice, having macrophages and NK cells but lacking both endogenous and infused T cells, SKV-012 (murine IL-12) treatment was also significantly more effective than oHSV or PBS control at inhibiting the progression of tumors (figure 4F, online supplemental figure S4), which was confirmed histologically both in animal model and human subjects in the subsequent clinical trial (online supplemental figures S5 and S6). Collectively, the data demonstrate that SKV-012 improves the efficacy of oncolytic virotherapy in vivo in multiple xenograft models.

Patient demographic

A total of six eligible subjects with advanced malignant solid tumors, who failed at least two standard lines of therapies (table 1), were enrolled and received intratumoral SKV-012 injection per protocol (online supplemental figure S7). All patients were adults, with three having stage IV squamous cell carcinoma (SCC) in the thigh, ear or larynx. Additionally, one patient (P002), diagnosed with skin SCC, also had bone metastasis in the femur. Two patients had stage IV melanoma in maxillary sinus and nuchae; both patients with melanoma experienced liver metastasis (online supplemental figure S8), while the patient with nuchae melanoma also had bone metastasis. One patient had recurrent stage IV soft tissue sarcoma of the right foot after surgery. All patients had ECOG scores of 1 and had a history of prior immune checkpoint inhibitor (ICI) use except patient 3.

Viral shedding

The patient's saliva, blood, urine, and stool samples were all negative for viral shedding at the 4-hour, 2-day, and 7-day time points, as determined by qPCR testing. Only the wound dressing yielded positive results at the 4-hour and 2-day time points. These findings suggest a favorable safety profile with no evidence of systemic viral infection (online supplemental table S3).

Safety

Treatment-related AEs were recorded during the treatment and follow-up period; grade 3 or higher AEs were not observed (table 2). In the low-dose group, the treatment-related AEs occurred in two of three subjects. P001 experienced a transient fever 2 hours after the second injection, which resolved after using ibuprofen. P001 also developed shingles around the neck 2 days after the third injection (online supplemental figure S9), which resulted in temporary cessation of the medication and the initiation of acyclovir treatment. Patient P001 also had mild anemia throughout the treatment course (online supplemental figure S10). P003 developed two episodes of dizziness within 1 hour after injection, which gradually resolved after bed rest. The hemoglobin level decreased to around 80 g/L at the 28th day after treatment initiation (online supplemental figure S11). In the high-dose group, the treatment-related AEs also occurred in two of three subjects. Subject P004 had mild transient fever and dizziness around 6 hours after the first injection, which were managed with ibuprofen. The hemoglobin level went down to 88 g/L 4 hours after initial treatment but went up to above 100 g/L on day 7 (online supplemental figure S12). Subject P005 had an injection site reaction, where the tissue around the needle hole bumped up and appeared reddish (online supplemental figure S13). No noticeable AEs occurred in subjects P002 and P006 (online supplemental figures S14 and S15). Findings indicated that AEs were mild, ensuring a satisfactory safety profile.

Treatment efficacy

Among the six subjects, three attained PR (figure 5A–D), one achieved SD (figure 5F), and two had PD after treatment (figure 5B,C).

Subjects P001, P003 and P004 exhibited 33.8%, 61.1% and 49.6% decrease in target lesion, respectively, which sustained for over 29 weeks for P001 and over 23 weeks for P003; the PR of P004 ended at the 29th week of evaluation. The liver metastasis of P001 also demonstrated

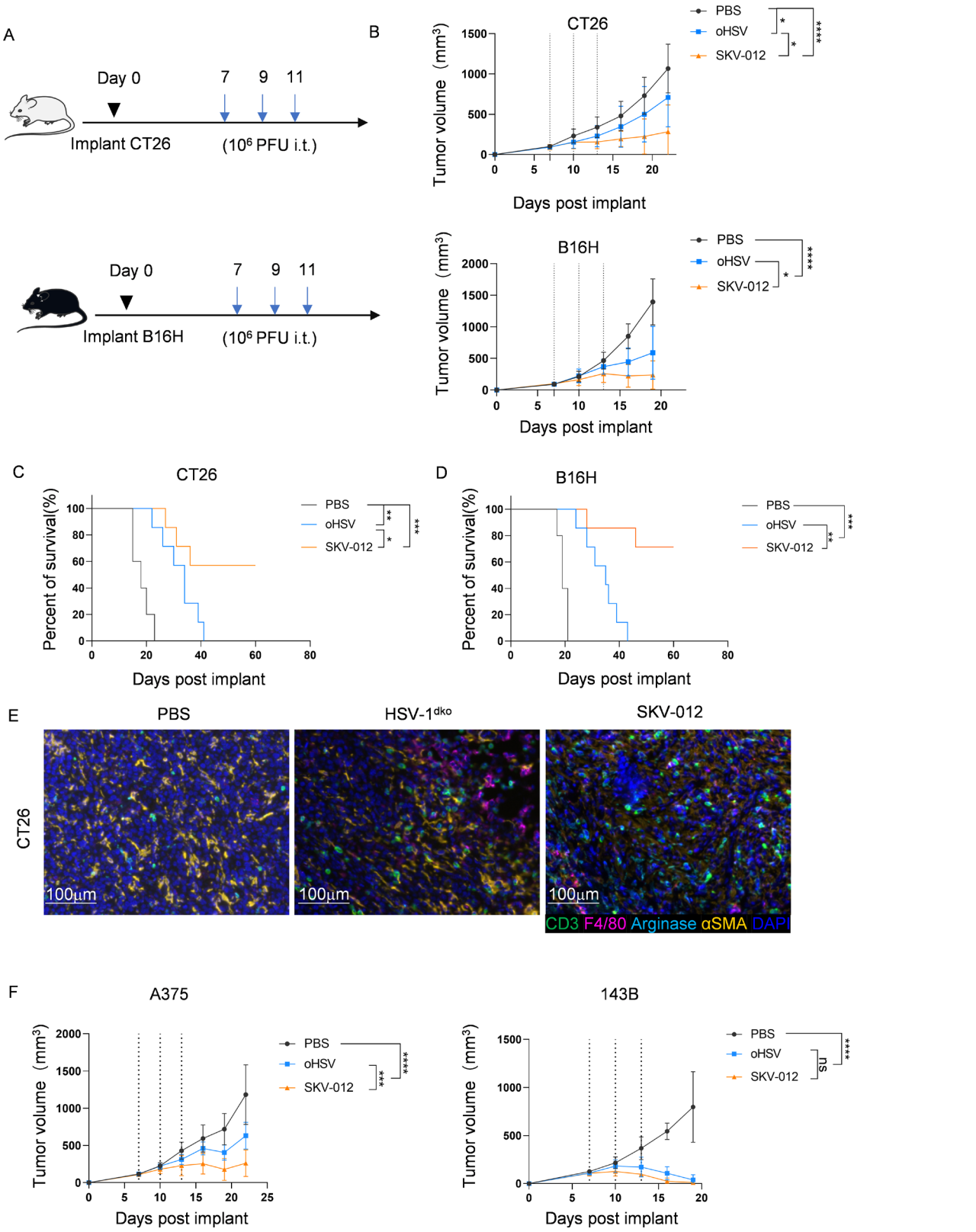


Figure 4 Animal experiments. (A) Treatment schematic. (B) Tumor responses (n=5/group). Data are mean±SD. Dashed vertical lines represent dosing days. (C, D) Survival rates of CT26 or B16H tumor-bearing mice treated with phosphate buffered saline (PBS), oHSV, or SKV-012 (murine IL-12). Survival rates were estimated by the Kaplan-Meier method and compared by the log-rank test (n=5–7 independent mice). (E) Multiplex immunohistochemistry (mIHC) imaging of cell populations in CT26. (F) Tumor volume changes in A375 or 143B xenograft models following intratumoral injections of PBS, oHSV or SKV-012 (murine IL-12) administered two times per week on a weekly schedule. Tumor response (n=5/group). Data are mean±SD. Dashed vertical lines represent dosing days. (B, F) Two-way analysis of variance (ANOVA) with Tukey's multiple comparison tests. ****P<0.0001, ***p<0.001, **p<0.01, *p<0.05; ns, p>0.05. IL, interleukin; oHSV, oncolytic herpesvirus.

Table 1 Baseline clinical characteristics of participants

ID	Pathology	Primary lesion	ECOG	Distant metastasis/local recurrence	Lines of prior therapy	Prior ICI therapy
P001	Stage IV Mel	Maxillary sinus	1	Liver	3	Y
P002	Stage IV SCC	Skin (thigh)	1	Bone	5	Y
P003	Stage IV STS	Foot	1	Foot	2	N
P004	Stage IV SCC	Larynx	1	Larynx	2	Y
P005	Stage IV Mel	Nuchae	1	Liver, bone	4	Y
P006	Stage IV SCC	Ear	1	Ear	2	Y

ECOG, Eastern Cooperative Oncology Group; ICI, immune checkpoint inhibitor; Mel, melanoma; N, no; SCC, squamous cell carcinoma; STS, soft tissue sarcoma; Y, yes.

a response to the OV (online supplemental figure S8A,B), and the patient's nasal hemorrhage due to melanoma was also relieved after treatment commencement (online supplemental figure S9C,D). Subject P005 experienced SD; however, the patient experienced PD in the liver metastasis at the second radiological evaluation on the 10th week after treatment commencement, and the patient refused further SKV-012 injections (online supplemental figure S8C). Subjects P002 and P006 with SCC both experienced PD at the first radiological evaluation on day 28; the non-injected metastatic lesions also progressed in subject P002.

In the first cycle of therapy, the anti-HSV antibody of each patient all trended upward with the ongoing treatment (figure 5E,F; online supplemental figure S16), indicating a gradual systemic resistance to the virus. The high-dose group exhibited higher mean anti-HSV antibody levels compared with the low-dose group (figure 5E). There was not much difference between the responder group (P001, P003 and P004) and the non-responder group (P002, P005, P006) (figure 5F). In terms of cytokine IL-12, one of the major functional products of the SKV-012 showed an upward trend in the first 2 days after administration and gradually trended down before the second dose in most of the patients (online supplemental figure S17A). Comparing responder and non-responder groups, the responder group had an overall higher IL-12 level, preferred viral activity or a stronger reaction against virus (figure 5G). IFN-γ increased right after the first injection but gradually decreased after the first dose (online supplemental figure S17B), while the responder group carried a slightly higher mean IFN-γ secretion than the non-responder group (figure 5H).

Single-cell transcriptome sequencing and mIHC

To study the changes in the tumor immune microenvironment after OV treatment, we obtained scRNA-seq data of fresh tumors from four patients before and after treatment, including 66 355 cells and 33 694 genes. We detected 15 cell clusters: B cell, CD4+ T cell, CD8+ T cell, conventional dendritic cell (cDC), cycling cell, endothelial cell, epithelial cell, macrophage, monocyte, mesenchymal stem cell, neutrophil, plasmacytoid DC, plasma cell, tumor-associated macrophage and Tregs, which were well distributed in the samples of all patients (figure 6A, online supplemental figure S18A,B). The results of the study showed that in pretreatment and post-treatment specimen analysis, there was a significant increase in cytotoxic T cells in responding patients compared with non-responders, as well as cDCs, which play an important

Table 2 Summary of treatment-related AEs

	Total		Cohort			
	n=6		Low (n=3)		High (n=3)	
Grade	1–2	≥3	1–2	≥3	1–2	≥3
Any events	4 (66.7%)	0	2 (66.7%)	0	2 (66.7%)	0
Fever	2 (33.3%)	0	1 (33.3%)	0	1 (33.3%)	0
Dizziness	2 (33.3%)	0	1 (33.3 %)	0	1 (33.3%)	0
Injection site reaction	1 (16.7%)	0	0	0	1 (33.3%)	0
Rash	1 (16.7%)	0	1 (33.3%)	0	0	0
Anemia	3 (50.0%)	0	2 (66.7%)	0	1 (33.3%)	

All data are presented as n (%).
Listed are events that were related to treatment by the investigators. The number of patients with treatment-related AEs was recorded after the initiation of virus therapy. These were all grade 1 or 2.
AE, adverse event.

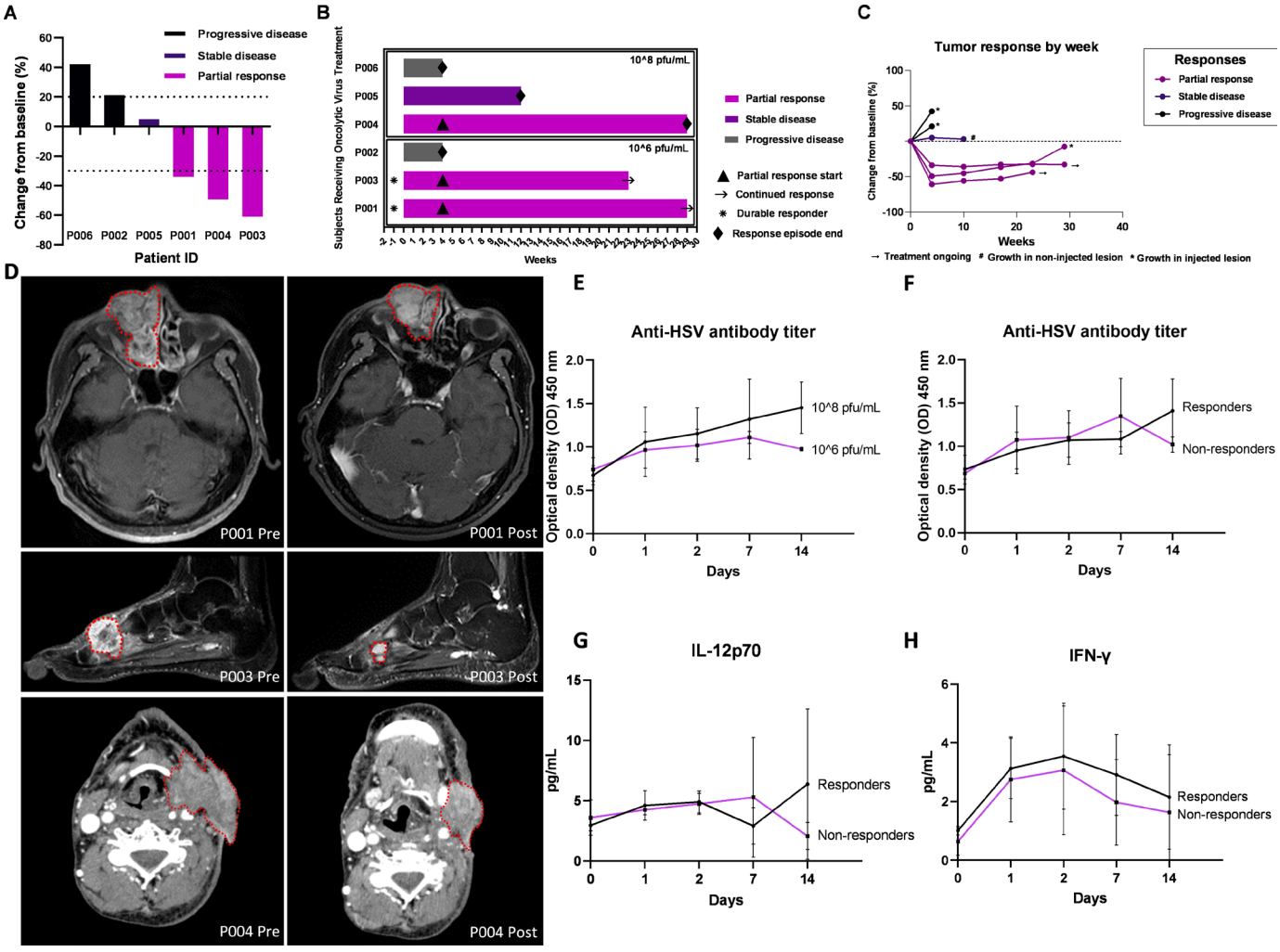


Figure 5 The detailed clinical results of the SKV-012 trial. (A, B, C) The waterfall, swimming and spider plot of treatment efficacy. (D) The pretreatment and post-treatment radiological comparison in patients with partial response. (E) The anti-HSV antibody level of the low-dose (10^6 pfu/mL) and high-dose (10^8 pfu/mL) group. Day 0 represents baseline condition. The blood sample on day 1 was collected 4 hours after injection, while the blood sample on day 14 was collected before the second virus injection (n=3). (F) The anti-HSV antibody level of responder and non-responder group (n=3). (G) The IL-12 level of responder and non-responder group (n=3). (H) The IFN-γ level of responder and non-responder group (n=3). HSV, herpes simplex virus; IFN-γ, interferon gamma; IL, interleukin.

role in antigen presentation (figure 6B,C). Frequency analysis revealed variation in the composition of clusters among patients. The results imply that the clinical response to OV therapy may be determined by cytotoxic T cell infiltration. In the CD8+ T cell subcluster, the cytotoxicity genes GZMA, GZMB, NKG7 and GNLY were significantly increased (figure 6D). Simultaneously, analysis of CellChat revealed widespread and intricate cell-to-cell communication, and the activation of CD8+ T cells, CD4+ T cells and B cells was significantly increased in the response group compared with the non-response group (figure 6E). Next, in order to identify changes in the TME during treatment, we used Monocle 2.0 to construct a pseudo-trajectory analysis of single cells, and the pseudo-time diagram showed that the post-treatment cells in the responsive or non-responsive group were in the late stage of cell trajectory development. In order to understand the linkages between different immune cells, the results of the potential developmental trajectories of the constructed associated immune cell clusters (B cells, CD8+ T cells, CD4+ T cells, and cDCs) suggested that the inferred developmental trajectories have yielded a branched structure in which cytotoxic T cells and B cells are located at one end of the mature cluster, and cytotoxic T cells are highly enriched in the terminal phase of the false time. Afterwards, we project gene expression for CD8A, CD8B, and CD4 onto pseudo-dating trajectories. It is worth noting that CD8A and CD8B genes (online supplemental figure S18C) increased significantly with the posterior shift of the pseudo-time, and the CD4 gene (online supplemental figure S18D) also increased. Collectively, during OV therapy, cytotoxic T cells are gradually activated, with a rich immune microenvironment, regulating the immune response.

The pretreatment and post-treatment mIHC was conducted on the target cancer lesion of subject P004,

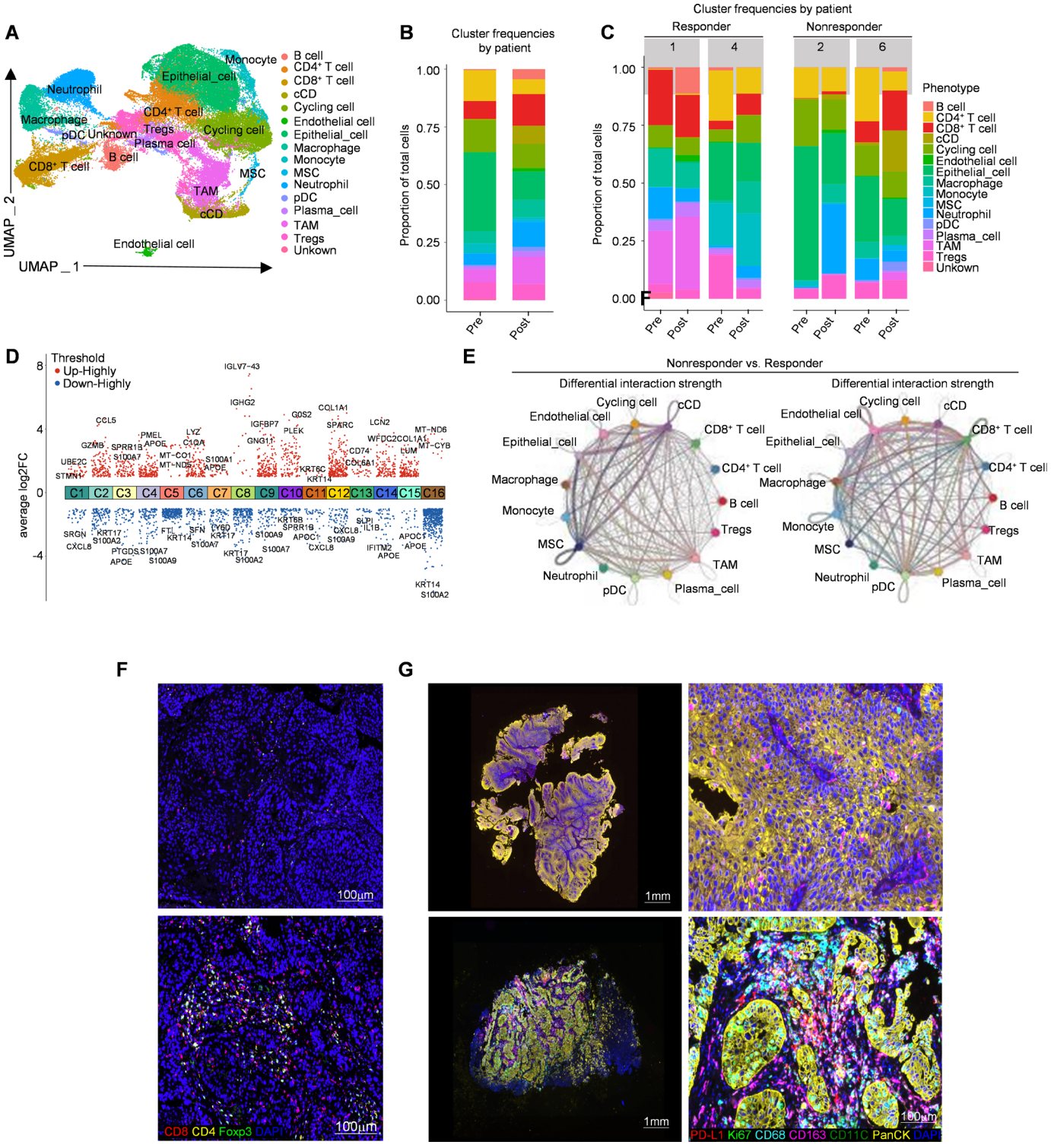


Figure 6 Single-cell analysis of changes in the tumor immune microenvironment of patients before and after treatment. (A) Uniform manifold approximation and projection (UMAP) plot shows the distribution of all cells in four patients with clusters, color-coded and labeled by annotated cell type. (B, C) Cluster frequencies by time point. Patients are separated into two groups: responders (patients 1 and 4) and non-responders (patients 2 and 6). (D) Volcano graphic showing differentially expressed genes (DEGs) in the immune cell subclusters that have been annotated. C1: cycling cells; C2: CD8+ T cells; C3: epithelial cells; C4: TAM; C5: Tregs; C6: macrophages; C7: plasma cells; C8: B cells; C9: endothelial cells; C10: neutrophils; C11: CD4+ T cells; C12: cDCs; C13: pDCs; C14: monocytes; C15: MSC; C16: unknown. (E) Comparison between responsive and non-responsive treatment groups of the various interaction intensities among 15 identified cell types. Strength of effect is indicated by line thickness. (F, G) The multiplex immunohistochemistry of the subject P004 staining PD-L1, Ki67, CD163, CD11C, PanCK, DAPI, and CD68. cDC, conventional dendritic cell; MSC, mesenchymal stem cell; pDC, plasmacytoid dendritic cell; TAM, tumor-associated macrophage.

who achieved and sustained the PR for 29 weeks. Various types of immune cells including CD68+ macrophage, CD163+ macrophage, CD11c+ DC, CD4+ T cell, and CD8+ T cell demonstrated a marked increase in infiltration in the post-treatment target lesion compared with the pretreatment sample (figure 6F,G, online supplemental figure S19), indicating an effective transformation of cold tumor into hot tumor by the SKV-012 (online supplemental figure S18E,F). The significant decrease in PanCK also indicated an overall good tumor response to the OV treatment. Intratumoral administration of SKV-012 increased immune cell infiltration into the tumor but also induced PD-L1 expression. The upregulation of PD-L1 indicates that the patient might benefit from the application of ICIs.

DISCUSSION

Compared with other OVs, HSV-1 has special characteristics and advantages for genetic modification for the purposes of cancer treatment. The genome is large, with 150 kbp, making it suitable for multiple genetic modifications for various purposes; the cell-to-cell spread of the virus is not affected by the circulating anti-HSV antibody, thereby ensuring the long-term treatment effectiveness.[33] In addition, antiviral medications like acyclovir enable the physician to effectively control the infection when the virus is causing unwanted severe adverse effects.[34] To date, several genetically modified mutants of HSV have been applied for the treatment of various types of solid tumors, including T-VEC, HF10, NV1020, HSV1716, OH2, and G47Δ, and are undergoing a series of clinical trials aimed at evaluating their safety and efficacy for future clinical translation. Among the above-mentioned agents, T-VEC stands as the most extensively used and scrutinized OV worldwide, having garnered approval for clinical application from both the US-FDA and the European Medicines Agency.[35] Also, it is the only OV that has completed phase III clinical trial.

Late-stage solid tumors pose a significant clinical challenge due to their resistance to conventional therapies. Though OVs offer a promising alternative therapy, the choices are limited. Efforts in developing novel OVs as well as enhancing their efficacy through combination strategies are crucial. Incorporating cytokine therapy with oncolytic virotherapy has exhibited great potential in preclinical experiments.[36]

Our study revealed that cytokines IL-7, IL-15, and IL-12 increased immune cell infiltration to a similar extent. IL-7 and IL-15 are known to enhance the proliferation and survival of T cells, and they have been tested in clinical trials on patients with advanced cancers.[37 38] In addition, IL-15 has been shown to induce robust expansion of peripheral CD8 T cells and NK cells.[39 40] Despite promising biological activity at well-tolerated doses, IL-7 and IL-15 have shown limited clinical benefit in a monotherapy setting. A possible explanation for the lack of tumor regression is that these cytokines do not induce potent effector functions in CD8 T cells.[41]

IL-12 has been indicated to be able to elicit significant antitumor effects through the activation of CTLs and NK cells when delivered to the TME.[17] Our findings demonstrate that IL-12 enhanced the antitumor efficacy of oHSV. This is consistent with previous studies highlighting the role of IL-12 in promoting antitumor immunity by stimulating NK cell and T cell activation.[42 43] The increased infiltration of immune cells, especially CD8 T cells and NK cells, observed in the oHSV+IL-12 group suggests that this combination effectively reshapes the TME, creating a favorable immune context for tumor eradication while boosting memory formation as assessed by tumor rechallenge experiments (figure 2B–D, online supplemental figure S2B). Further studies are required to explore additional mechanisms, such as specific phenotypes of the T cell infiltrate, landscape of tumor-draining lymph node, and antigen processing and presentation pathways, which may contribute to the superior efficacy of IL-12.

To further enhance the oncolytic potential of oHSV, we developed SKV-012, which incorporates an IL-12 transgene driven by the CMV promoter and ICP34.5 under the Survivin promoter. Survivin, an antiapoptotic protein overexpressed in many cancers,[44] served as a suitable promoter for driving ICP34.5 expression, a key virulence factor essential for efficient viral replication in tumor cells. The incorporation of IL-12 into SKV-012 aimed to augment the virus's immunomodulatory properties. Our in vitro data demonstrated that SKV-012 exhibited relatively enhanced viral replication, cytotoxicity, and IL-12 production compared with the parental oHSV. These findings suggest that SKV-012 possesses improved oncolytic and immunogenic properties.

The in vivo studies revealed that SKV-012 demonstrated superior antitumor efficacy compared with oHSV alone in both immunocompetent and immunodeficient mouse models, further evidencing its ability to stimulate antitumor immune responses. There was no significant difference in weight changes in SKV-012-treated mice, suggesting that the local delivery of IL-12 from the virus may mitigate systemic toxicity associated with high-dose IL-12 administration.[42]

After the verification of safety and efficacy of SKV-012 in animal models, we started the phase I clinical trial to investigate the safety and preliminary efficacy of the SKV-012 in human subjects. We found that repeated intratumoral injection of 10^8 pfu/mL up to 4 mL is safe with no reported severe adverse effects (grade ≥3). Early trials of oncolytic HSV found that two concentrations at 10^6 and 10^8 pfu were sufficient to cover the effective dose range, while considering the balance between safety and efficacy. Additionally, since OVs are administered via intratumoral injection, resulting in high local concentrations and low systemic toxicity, multiple concentrations may not be necessary. Also, according to prior HSV-based studies, the tested concentration mainly lies between 10^6 and 10^8 pfu,[34 45 46] so we decided to recruit only two

concentration groups with the maximal concentration set at 10^8 pfu. The most frequent adverse effects caused by SKV-012 were mild anemia, transient fever and dizziness, which are consistent with the report from other clinical trials on HSV-based OVs.[2 46] The anemia can be managed through enhanced nutritional support, while fever can be effectively managed by antipyretics. The absence of IL-12-related adverse effects proved that the local delivery of IL-12 can effectively mitigate systemic toxicity. The absence of grade 3 or higher toxicities supports a favorable safety profile for further clinical development. The biodistribution of the SKV-012 also indicated that the agent is safe and unlikely to spread through saliva, urine or feces.

Meanwhile, a proportion of patients exhibited objective tumor responses. Durable responses were observed in patients with melanoma, soft tissue sarcoma and SCC. In addition, the metastatic melanoma lesion also showed a response to the OV; the abscopal effect demonstrated the mechanism of oncolytic virotherapy with SKV-012 capable of eradicating distant malignancies via tumor-selective infection or immune responses. The elevated peripheral IL-12 levels indicated that the SKV-012 offers an effective means for targeted delivery and expression of IL-12 within the TME; the increased IFN-γ further demonstrated the effectiveness of SKV-012 in recruiting and activating CD4+ T cells, CD8+ T cells, and NK cells. The overall safety and efficacy profile indicated that the SKV-012 is an OV of great potential in solid tumor treatment and is promising for clinical translation. We also observed a phenomenon that in the SD and PD patients, though the IL-12 and IFN-γ expression was no different from PR patients, the treatment efficacy is suboptimal. For non-responders, they generally have more bulky tumors than patients with PR. We hypothesize that larger tumors may present a greater challenge for OVs due to more excessive and denser extracellular matrix deposition and disorganized vascular architecture,[47] thereby hindering immune cell recruitment.

The study of pretreatment and post-treatment TME revealed a significant increase in cytotoxic T cells, particularly CD8+ T cells, in responding patients. This phenomenon aligns with the established role of cytotoxic T cells in mediating antitumor immunity.[48] Additionally, the enrichment of cDCs suggests a potential role in antigen presentation and T cell activation. These data collectively supported the hypothesis that the clinical response to SKV-012 therapy is associated with robust cytotoxic T cell infiltration and a favorable TME. Beyond the increase in cytotoxic T cells, the scRNA-seq analysis revealed a broader shift in the TME towards a more activated and immunogenic phenotype. The upregulation of cytotoxicity genes within the CD8+ T cell subcluster and the enhanced cell-to-cell communication among immune cells suggest a coordinated immune response elicited by SKV-012. The TME shift was further evidenced by the mIHC analysis of patient P004, which confirmed the findings from the scRNA-seq data, demonstrating increased infiltration of various immune cell types and a reduction in tumor markers in the post-treatment tumor. Inhibitory factors like PD-L1 were also elevated, which could be attributed to the upregulation of inflammatory signaling pathways, especially Interferon-γ/Janus Kinase/Signal Transducer and Activator of Transcription-1 (IFN-γ/JAK/STAT1) pathway, due to the significant increase in circulating IFN-γ in P004, which effectively upregulates PD-L1 mRNA expression.[49] The presence of PD-L1 often serves as a biomarker to predict the efficacy of anti-PD-1 therapies; higher levels of PD-L1 expression on tumor cells can correlate with better responses to anti-PD-1 therapies, thereby indicating the potential combination therapy with anti-PD-1 medications.[50] Similar combination designs have demonstrated preferred treatment efficacy in T-VEC and OH2 trials.[46 51]

The OV SKV-012, a novel combination of IL-12-expressing HSV and a tumor-specific Survivin promoter, represents the first reported combination of a cytokine-expressing HSV with a tumor-specific promoter. As such, it is also the first of its kind to undergo clinical trials in human subjects. It demonstrates promising efficacy and safety in phase I clinical trials. The Survivin promoter ensures targeted activation of the virulence factors of HSV within tumor cells, leading to enhanced antitumor activity. In theory, SKV-012 offers several advantages over FDA-approved OVs like T-VEC. First, the Survivin promoter, which is highly active in many tumor types but minimally expressed in normal tissues, may improve tumor selectivity and reduce off-target toxicity.[52] Meanwhile, the expression of IL-12 could further enhance antitumor immune response by activating T cells and NK cells, potentially leading to systemic immune-mediated tumor control.[21] In contrast, T-VEC relies primarily on its ability to replicate in tumor cells and locally stimulate DC maturation and antigen presentation, while the immune stimulation efficacy can be hindered by immunosuppressive TME. However, SKV-012 is still in its very early stages of development, with only phase I clinical trial done so far, meaning its actual efficacy remains somehow unproven compared with the well-established clinical profile of T-VEC.

In the future development of OVs with cytokine therapy incorporated, a recent study with exceptional delivery design could be referenced. Chiocca *et al* conducted a multicenter clinical trial on regulated hIL-12 in recurrent advanced glioma. They propose a RheoSwitch system that uses adenovirus vector to deliver the IL-12 (Ad-RTS-hIL-12) while regulating the IL-12 expression by oral veledimex (VDX). Such a system allows precise transcriptional control so that IL-12 is produced locally only when VDX is administered, minimizing off-target effects. Moreover, VDX crosses the blood-brain barrier, achieving intratumoral IL-12 expression while permitting dose-dependent regulation, which resulted in minimized systemic toxicity and good survival outcomes.[53] This design strategy could be adapted to our future virus design in order to induce a prolonged immune response even after the virus is cleared from the tumor.

While the initial results of this study are encouraging, the small sample size and variability in tumor types necessitate further evaluation. Additionally, exploring the potential benefits of combining SKV-012 with other therapies, such as ICIs, could further enhance its therapeutic potential. Certain clinical trials have explored the efficacy of combinatorial therapy involving ICIs and OVs. These studies have demonstrated that the combination enhances antitumor immune responses, leading to improved tumor control and increased survival rates.[54 55] Additionally, OVs have shown potential in overcoming resistance to ICIs, further expanding their therapeutic utility.[56] By addressing these limitations and expanding on the initial findings, SKV-012 could become a valuable tool in the fight against cancer.

To conclude, SKV-012, a novel OV expressing IL-12, demonstrates a favorable safety profile and promising therapeutic potential for advanced solid tumors. Despite patients' resistance to conventional treatments, SKV-012 induced encouraging responses. By effectively reshaping the TME, SKV-012 could offer a promising avenue for cancer immunotherapy.

Author affiliations
[1]Department of Biotherapy, Cancer Center, Sichuan University West China Hospital, Chengdu, Sichuan, China
[2]State Key Laboratory of Biotherapy and Cancer Center, Research Unit of Gene and Immunotherapy, Chinese Academy of Medical Sciences, Collaborative Innovation Center of Biotherapy, West China Hospital of Sichuan University, Chengdu, Sichuan, China
[3]Fifth People's Hospital of Ningxia Hui Autonomous Region, Shizuishan, Ningxia, China
[4]Department of Neurosurgery, West China Hospital of Sichuan University, Chengdu, Sichuan, China
[5]Department of Neurosurgery, NHC Key Laboratory of Nuclear Technology Medical Transformation (Mianyang Central Hospital), School of Medicine, University of Electronic Science and Technology of China, Mianyang, Sichuan, China
[6]Department of Otolaryngology- Head & Neck Surgery, West China Hospital of Sichuan University, Chengdu, China
[7]Cancer Prevention and Treatment Institute of Chengdu, Department of Oncology, Chengdu Fifth People's Hospital (The Second Clinical Medical College,Affiliated Fifth People's Hospital of Chengdu University of Traditional Chinese Medicine), Chengdu, Sichuan, China
[8]State Key Laboratory of Biotherapy and Cancer Center, West China Hospital of Medicine, Chengdu, China
[9]Frontiers Medical Center, Tianfu Jincheng Laboratory, Chengdu, Sichuan, China

Acknowledgements We thank all the patients, their families and the site investigators who participated in this study.

Contributors XP is the guarantor of this study. Conceptualization: XP and AT. Methodology: ZJ, NY, JJ, LJ, ZZ and HL. Investigation: ZJ, NY, JJ, ZZ, HL, LX, YC, WZ, HY, and JL. Visualization: ZJ, NY, JJ, ZZ, HL, LX, YC, HY, WZ, JL, XP and AT. Funding acquisition: XP and AT. Project administration: ZJ, NY, LZ and JJ. Supervision: XP, HY, JL, LZ and AT. Writing—original draft: ZJ, NY and JJ. Writing—review and editing: ZJ, NY, JJ, ZZ, HL, LX, YC, HY, JL XP and AT.

Funding This work was supported by funding from the National Natural Science Foundation of China (32471551, 82473434), the National Key Research and Development Program of China (2023YFC3403303 and 2023YFC3403304), the Frontiers Medical Center, Tianfu Jincheng Laboratory Foundation (TFJC2023010006), the Major Scientific and Technological Achievements Transformation Project, Ningxia Hui Autonomous Region (2022CJE09013), the National Key Research and Development Program of China (2021YFE0206600), Sichuan Provincial Science and Technology Department Key Research and Development Program (2022YFSY0012), Sichuan Science and Technology Program (2024YFHZ0041, 2024ZYD0054), Science and Technology Project of Sichuan Provincial Health Commission (Clinical Research Special Project JH2023082), the International Science and Technology Cooperation Program of Chengdu Science and Technology Bureau (2024-YF06-00011-HZ and 2022-GH03-00004-HZ), the Strategic Cooperation Special Fund of Sichuan University-Dazhou Municipal People's Government (2021CDDZ-25, 2022CDDZ-16), the Science and Technology Cooperation Special Fund of Sichuan University-Zigong (2021CDZG-24), the Health Research Project of Chengdu Eastern New Area Management Committee (202304), 1.3.5 Project for Disciplines of Excellence from West China Hospital of Sichuan University (ZYYC23006), the Achievement Transformation Fund of West China Hospital (CGZH19002), the Clinical Research Incubation Project of West China Hospital (23HXFH001), and the Ministry of Education University-Industry Collaborative Education Program (230720523707281).

Disclaimer The funders had no role in study design, data collection and analysis, decision to publish, or preparation of the manuscript.

Competing interests None declared.

Patient consent for publication Consent obtained directly from patient(s).

Ethics approval This study involves human participants and was approved by the Institutional Review Board of West China Hospital (reference number: 2023-833). The informed consent has been obtained directly from the patients and the families. Participants gave informed consent to participate in the study before taking part.

Provenance and peer review Not commissioned; externally peer reviewed.

Data availability statement Data are available upon reasonable request.

Supplemental material This content has been supplied by the author(s). It has not been vetted by BMJ Publishing Group Limited (BMJ) and may not have been peer-reviewed. Any opinions or recommendations discussed are solely those of the author(s) and are not endorsed by BMJ. BMJ disclaims all liability and responsibility arising from any reliance placed on the content. Where the content includes any translated material, BMJ does not warrant the accuracy and reliability of the translations (including but not limited to local regulations, clinical guidelines, terminology, drug names and drug dosages), and is not responsible for any error and/or omissions arising from translation and adaptation or otherwise.

Open access This is an open access article distributed in accordance with the Creative Commons Attribution Non Commercial (CC BY-NC 4.0) license, which permits others to distribute, remix, adapt, build upon this work non-commercially, and license their derivative works on different terms, provided the original work is properly cited, appropriate credit is given, any changes made indicated, and the use is non-commercial. See http://creativecommons.org/licenses/by-nc/4.0/.

ORCID iDs
Zheng Jiang http://orcid.org/0000-0001-7160-4512
Hui Yang http://orcid.org/0000-0003-0039-4364
Aiping Tong http://orcid.org/0000-0002-3392-5443
Xingchen Peng http://orcid.org/0000-0001-7042-718X

REFERENCES

1 Kelly E, Russell SJ. History of oncolytic viruses: genesis to genetic engineering. *Mol Ther* 2007;15:651–9.
2 Hu JCC, Coffin RS, Davis CJ, *et al*. A phase I study of OncoVEXGM-CSF, a second-generation oncolytic herpes simplex virus expressing granulocyte macrophage colony-stimulating factor. *Clin Cancer Res* 2006;12:6737–47.
3 Lundstrom K. Viral Vectors in Gene Therapy: Where Do We Stand in 2023? *Viruses* 2023;15:698.
4 Tomazin R, van Schoot NE, Goldsmith K, *et al*. Herpes simplex virus type 2 ICP47 inhibits human TAP but not mouse TAP. *J Virol* 1998;72:2560–3.
5 Kohlhapp FJ, Kaufman HL. Molecular Pathways: Mechanism of Action for Talimogene Laherparepvec, a New Oncolytic Virus Immunotherapy. *Clin Cancer Res* 2016;22:1048–54.
6 Toda M, Martuza RL, Rabkin SD. Tumor growth inhibition by intratumoral inoculation of defective herpes simplex virus vectors expressing granulocyte-macrophage colony-stimulating factor. *Mol Ther* 2000;2:324–9.
7 Zhang T, Jou TH-T, Hsin J, *et al*. Talimogene Laherparepvec (T-VEC): A Review of the Recent Advances in Cancer Therapy. *J Clin Med* 2023;12:1098.
8 Andtbacka RHI, Collichio F, Harrington KJ, *et al*. Final analyses of OPTiM: a randomized phase III trial of talimogene laherparepvec versus granulocyte-macrophage colony-stimulating factor in

unresectable stage III-IV melanoma. *J Immunother Cancer* 2019;7:145.
9 Harrington KJ, Kong A, Mach N, *et al*. Talimogene Laherparepvec and Pembrolizumab in Recurrent or Metastatic Squamous Cell Carcinoma of the Head and Neck (MASTERKEY-232): A Multicenter, Phase 1b Study. *Clin Cancer Res* 2020;26:5153–61.
10 Guo ZS, Bartlett DL. Oncolytic viruses as platform for multimodal cancer therapeutics: a promising land. *Cancer Gene Ther* 2014;21:261–3.
11 Sova P, Ren X-W, Ni S, *et al*. A tumor-targeted and conditionally replicating oncolytic adenovirus vector expressing TRAIL for treatment of liver metastases. *Mol Ther* 2004;9:496–509.
12 Liu Z, Ge Y, Wang H, *et al*. Modifying the cancer-immune set point using vaccinia virus expressing re-designed interleukin-2. *Nat Commun* 2018;9:4682.
13 Wong RJ, Chan M-K, Yu Z, *et al*. Angiogenesis inhibition by an oncolytic herpes virus expressing interleukin 12. *Clin Cancer Res* 2004;10:4509–16.
14 Kowalsky SJ, Liu Z, Feist M, *et al*. Superagonist IL-15-Armed Oncolytic Virus Elicits Potent Antitumor Immunity and Therapy That Are Enhanced with PD-1 Blockade. *Mol Ther* 2018;26:2476–86.
15 Weiss T, Puca E, Silginer M, *et al*. Immunocytokines are a promising immunotherapeutic approach against glioblastoma. *Sci Transl Med* 2020;12:eabb2311.
16 Portielje JEA, Gratama JW, van Ojik HH, *et al*. IL-12: a promising adjuvant for cancer vaccination. *Cancer Immunol Immunother* 2003;52:133–44.
17 Brunda MJ, Luistro L, Warrier RR, *et al*. Antitumor and antimetastatic activity of interleukin 12 against murine tumors. *J Exp Med* 1993;178:1223–30.
18 Nguyen KG, Vrabel MR, Mantooth SM, *et al*. Localized Interleukin-12 for Cancer Immunotherapy. *Front Immunol* 2020;11:575597.
19 Vo JL, Yang L, Kurtz SL, *et al*. Neoadjuvant immunotherapy with chitosan and interleukin-12 to control breast cancer metastasis. *Oncoimmunology* 2014;3:e968001.
20 Smith SG, Koppolu BP, Ravindranathan S, *et al*. Intravesical chitosan/interleukin-12 immunotherapy induces tumor-specific systemic immunity against murine bladder cancer. *Cancer Immunol Immunother* 2015;64:689–96.
21 Lasek W, Zagożdżon R, Jakobisiak M. Interleukin 12: still a promising candidate for tumor immunotherapy? *Cancer Immunol Immunother* 2014;63:419–35.
22 Jaiswal PK, Goel A, Mittal RD. Survivin: A molecular biomarker in cancer. *Indian J Med Res* 2015;141:389–97.
23 Chung RY, Saeki Y, Chiocca EA. B-myb promoter retargeting of herpes simplex virus gamma34.5 gene-mediated virulence toward tumor and cycling cells. *J Virol* 1999;73:7556–64.
24 Kambara H, Okano H, Chiocca EA, *et al*. An oncolytic HSV-1 mutant expressing ICP34.5 under control of a nestin promoter increases survival of animals even when symptomatic from a brain tumor. *Cancer Res* 2005;65:2832–9.
25 Ling AL, Solomon IH, Landivar AM, *et al*. Clinical trial links oncolytic immunoactivation to survival in glioblastoma. *Nature New Biol* 2023;623:157–66.
26 Zhang Z, Yang N, Lu H, *et al*. Improved antitumor effects elicited by an oncolytic HSV-1 expressing a novel B7H3nb/CD3 BsAb. *Cancer Lett* 2024;588:216760.
27 Friedman GK, Johnston JM, Bag AK, *et al*. Oncolytic HSV-1 G207 Immunovirotherapy for Pediatric High-Grade Gliomas. *N Engl J Med* 2021;384:1613–22.
28 Sweeney JG, Liang J, Antonopoulos A, *et al*. Loss of GCNT2/I-branched glycans enhances melanoma growth and survival. *Nat Commun* 2018;9:3368.
29 Hewitt SL, Bailey D, Zielinski J, *et al*. Intratumoral IL12 mRNA Therapy Promotes TH1 Transformation of the Tumor Microenvironment. *Clin Cancer Res* 2020;26:6284–98.
30 Ryncarz AJ, Goddard J, Wald A, *et al*. Development of a high-throughput quantitative assay for detecting herpes simplex virus DNA in clinical samples. *J Clin Microbiol* 1999;37:1941–7.
31 Liu BL, Robinson M, Han Z-Q, *et al*. ICP34.5 deleted herpes simplex virus with enhanced oncolytic, immune stimulating, and anti-tumour properties. *Gene Ther* 2003;10:292–303.
32 Todo T, Ino Y, Ohtsu H, *et al*. A phase I/II study of triple-mutated oncolytic herpes virus G47Δ in patients with progressive glioblastoma. *Nat Commun* 2022;13:4119.
33 Cifuentes-Munoz N, El Najjar F, Dutch RE. Viral cell-to-cell spread: Conventional and non-conventional ways. *Adv Virus Res* 2020;108:85–125.
34 Nakao A, Kasuya H, Sahin TT, *et al*. A phase I dose-escalation clinical trial of intraoperative direct intratumoral injection of HF10 oncolytic virus in non-resectable patients with advanced pancreatic cancer. *Cancer Gene Ther* 2011;18:167–75.
35 Mondal M, Guo J, He P, *et al*. Recent advances of oncolytic virus in cancer therapy. *Hum Vaccin Immunother* 2020;16:2389–402.
36 Bommareddy PK, Wakimoto H, Martuza RL, *et al*. Oncolytic herpes simplex virus expressing IL-2 controls glioblastoma growth and improves survival. *J Immunother Cancer* 2024;12:e008880.
37 Fry TJ, Mackall CL. Interleukin-7: master regulator of peripheral T-cell homeostasis? *Trends Immunol* 2001;22:564–71.
38 Adachi K, Kano Y, Nagai T, *et al*. IL-7 and CCL19 expression in CAR-T cells improves immune cell infiltration and CAR-T cell survival in the tumor. *Nat Biotechnol* 2018;36:346–51.
39 Liu E, Marin D, Banerjee P, *et al*. Use of CAR-Transduced Natural Killer Cells in CD19-Positive Lymphoid Tumors. *N Engl J Med* 2020;382:545–53.
40 Berrien-Elliott MM, Becker-Hapak M, Cashen AF, *et al*. Systemic IL-15 promotes allogeneic cell rejection in patients treated with natural killer cell adoptive therapy. *Blood* 2022;139:1177–83.
41 Kang S, Mansurov A, Kurtanich T, *et al*. Engineered IL-7 synergizes with IL-12 immunotherapy to prevent T cell exhaustion and promote memory without exacerbating toxicity. *Sci Adv* 2023;9:eadh9879.
42 Xue D, Moon B, Liao J, *et al*. A tumor-specific pro-IL-12 activates preexisting cytotoxic T cells to control established tumors. *Sci Immunol* 2022;7:eabi6899.
43 Xu Y, Sun X, Tong Y. Interleukin-12 in multimodal tumor therapies for induction of anti-tumor immunity. *Discov Oncol* 2024;15:170.
44 Yang L, Cao Z, Li F, *et al*. Tumor-specific gene expression using the survivin promoter is further increased by hypoxia. *Gene Ther* 2004;11:1215–23.
45 Kemeny N, Brown K, Covey A, *et al*. Phase I, open-label, dose-escalating study of a genetically engineered herpes simplex virus, NV1020, in subjects with metastatic colorectal carcinoma to the liver. *Hum Gene Ther* 2006;17:1214–24.
46 Zhang B, Huang J, Tang J, *et al*. Intratumoral OH2, an oncolytic herpes simplex virus 2, in patients with advanced solid tumors: a multicenter, phase I/II clinical trial. *J Immunother Cancer* 2021;9:e002224.
47 Melssen MM, Sheybani ND, Leick KM, *et al*. Barriers to immune cell infiltration in tumors. *J Immunother Cancer* 2023;11:e006401.
48 Xie Q, Ding J, Chen Y. Role of $CD8^+$ T lymphocyte cells: Interplay with stromal cells in tumor microenvironment. *Acta Pharm Sin B* 2021;11:1365–78.
49 Garcia-Diaz A, Shin DS, Moreno BH, *et al*. Interferon Receptor Signaling Pathways Regulating PD-L1 and PD-L2 Expression. *Cell Rep* 2017;19:1189–201.
50 Davis AA, Patel VG. The role of PD-L1 expression as a predictive biomarker: an analysis of all US Food and Drug Administration (FDA) approvals of immune checkpoint inhibitors. *J Immunother Cancer* 2019;7:278.
51 Chesney JA, Puzanov I, Collichio FA, *et al*. Talimogene laherparepvec in combination with ipilimumab versus ipilimumab alone for advanced melanoma: 5-year final analysis of a multicenter, randomized, open-label, phase II trial. *J Immunother Cancer* 2023;11:e006270.
52 Chen J-S, Liu J-C, Shen L, *et al*. Cancer-specific activation of the survivin promoter and its potential use in gene therapy. *Cancer Gene Ther* 2004;11:740–7.
53 Chiocca EA, Yu JS, Lukas RV, *et al*. Regulatable interleukin-12 gene therapy in patients with recurrent high-grade glioma: Results of a phase 1 trial. *Sci Transl Med* 2019;11:eaaw5680.
54 Ribas A, Dummer R, Puzanov I, *et al*. Oncolytic Virotherapy Promotes Intratumoral T Cell Infiltration and Improves Anti-PD-1 Immunotherapy. *Cell* 2017;170:1109–19.
55 Desjardins A, Gromeier M, Herndon JE 2nd, *et al*. Recurrent Glioblastoma Treated with Recombinant Poliovirus. *N Engl J Med* 2018;379:150–61.
56 Zamarin D, Holmgaard RB, Subudhi SK, *et al*. Localized oncolytic virotherapy overcomes systemic tumor resistance to immune checkpoint blockade immunotherapy. *Sci Transl Med* 2014;6:226ra32.